



## Effect of chloride on Cu corrosion in anaerobic sulphide solutions

J. Chen, Z. Qin, T. Martino & D. W. Shoesmith

To cite this article: J. Chen, Z. Qin, T. Martino & D. W. Shoesmith (2017) Effect of chloride on Cu corrosion in anaerobic sulphide solutions, Corrosion Engineering, Science and Technology, 52:sup1, 40-44, DOI: [10.1080/1478422X.2016.1271161](https://doi.org/10.1080/1478422X.2016.1271161)

To link to this article: <https://doi.org/10.1080/1478422X.2016.1271161>



© 2017 The Author(s). Published by Informa UK Limited, trading as Taylor & Francis Group



Published online: 23 Aug 2017.



Submit your article to this journal [↗](#)



Article views: 113



View related articles [↗](#)



View Crossmark data [↗](#)



Citing articles: 1 View citing articles [↗](#)

## Effect of chloride on Cu corrosion in anaerobic sulphide solutions

J. Chen<sup>a,b</sup>, Z. Qin<sup>a</sup>, T. Martino<sup>a</sup> and D. W. Shoesmith<sup>a,b</sup>

<sup>a</sup>Department of Chemistry, The University of Western Ontario, London, Canada; <sup>b</sup>Surface Science Western, The University of Western Ontario, London, Canada

### ABSTRACT

The effect of chloride on copper corrosion in anaerobic aqueous sulphide solutions has been investigated using corrosion potential measurements, electrochemical impedance spectroscopy, scanning electron microscopy, focused ion beam and inductively coupled plasma atomic emission spectroscopy. Long-term exposure experiments were performed in  $10^{-3}$  mol L<sup>-1</sup> Na<sub>2</sub>S solutions containing chloride concentrations in a range from 0.1 to 5 mol L<sup>-1</sup>. Chloride was found to (i) inhibit Cu<sub>2</sub>S film growth by displacing adsorbed sulphide from the Cu surface; (ii) induce film porosity; (iii) facilitate transport of Cu<sup>+</sup> to the solution (at very high chloride concentrations).

### ARTICLE HISTORY

Received 23 November 2016  
Revised 23 November 2016  
Accepted 7 December 2016

### KEYWORDS

Copper; sulphide; corrosion; film; nuclear waste disposal

*This paper is part of a supplement on the 6th International Workshop on Long-Term Prediction of Corrosion Damage in Nuclear Waste Systems.*

### Introduction

Since copper is highly corrosion resistant and thermodynamically stable in the anoxic saline groundwater anticipated in deep geologic nuclear waste repositories, it is the candidate material for the manufacture of high level nuclear waste containers in Sweden, Finland and Canada [1–3]. Once oxygen, trapped in the repository on sealing, is consumed by microbial activity and mineral reactions in the bentonite clay compacted around the container, and by minor container corrosion, the major threat to the long-term durability of the container is corrosion by sulphide (SH<sup>-</sup>) produced in the groundwater by mineral dissolution and/or microbial activity involving sulphate-reducing bacteria [4,5]. For Swedish repository conditions, [SH<sup>-</sup>] is expected to be in the range  $10^{-7}$  to  $10^{-4}$  mol L<sup>-1</sup>, while [Cl<sup>-</sup>] can be up to 0.5 mol L<sup>-1</sup>.

Our previous work [6–8] showed that the corrosion product deposit formed on a Cu surface in anaerobic sulphide solutions in a range from  $5 \times 10^{-5}$  to  $10^{-3}$  mol L<sup>-1</sup> is a single layer Cu<sub>2</sub>S (chalcocite) film. Film growth occurs at the Cu<sub>2</sub>S/solution interface and is controlled by a combination of Cu<sup>+</sup> diffusion in the film and SH<sup>-</sup> diffusion in solution. In stagnant solutions with a low [Cl<sup>-</sup>]/[SH<sup>-</sup>] ratio ( $\leq 500$ ), the film appears compact, and its growth obeys a parabolic law. Under these circumstances, film growth is controlled mainly by Cu<sup>+</sup> diffusion in the Cu<sub>2</sub>S film indicating the film is protective. However, when the [Cl<sup>-</sup>]/[SH<sup>-</sup>] ratio is  $\geq 1000$ , the film has a cellular structure and its growth kinetics are linear. The film growth process is controlled primarily by SH<sup>-</sup> diffusion in solution, implying that the Cu<sub>2</sub>S film is not protective under these conditions [9]. These results suggest that the properties of the Cu<sub>2</sub>S film formed in anaerobic SH<sup>-</sup> solutions not only depend on [SH<sup>-</sup>] and [Cl<sup>-</sup>] but also on their ratio. However, when convection is involved, the properties of the Cu<sub>2</sub>S film are determined by the relative rates of diffusive sulphide flux and the interfacial reaction leading to the deposition of Cu<sub>2</sub>S [10].

The aim of the present study is to clarify the role of Cl<sup>-</sup> in the formation of the Cu<sub>2</sub>S films in stagnant anaerobic SH<sup>-</sup> solutions containing Cl<sup>-</sup>. A longer term goal is to determine whether the structure and properties of the sulphide films are determined by the SH<sup>-</sup> flux at the Cu<sub>2</sub>S/solution interface [10] or by the [Cl<sup>-</sup>]/[SH<sup>-</sup>] ratio.

### Experimental

#### Sample preparation

All experiments were performed with phosphorous-doped (30–100 ppm), oxygen-free Cu (Cu-OF) provided by the Swedish Nuclear Fuel and Waste Management Co. (SKB), Stockholm, Sweden. Working electrodes were Cu discs, with a diameter of 1 cm, threaded onto a stainless steel shaft painted with a non-conductive lacquer to prevent contact of the Cu/steel junction with the aqueous solution. After painting, electrodes were heated at 60°C for 12 h to promote adhesion between the paint and the sample. Copper surfaces were ground successively with 240, 600, 800, 1000, 1200 grade SiC paper and then polished to a mirror finish using 1, 0.3, and 0.05  $\mu$ m Al<sub>2</sub>O<sub>3</sub> suspensions. Before experiments, electrodes were washed with Type I water (ASTM D1193-6) with a resistivity of 18.2 M $\Omega$ cm (obtained from a Thermo Scientific Barnstead Nanopure 7143 ultrapure water system), cleaned using methanol (reagent grade), washed again with Type I water, and finally dried using ultra-pure Ar.

#### Electrochemical experiments

All experiments were performed in an Ar-purged anaerobic chamber (Canadian Vacuum Systems Ltd), maintained at a positive pressure (2–4 mbar) by an MBraun glove box control system, to ensure anoxic conditions were maintained (CO<sub>2</sub> < 1 ppm). The [O<sub>2</sub>] in the chamber was analysed with an MBraun O<sub>2</sub> probe.

Electrodes were exposed to a  $10^{-3}$  mol L $^{-1}$  Na $_2$ S solution containing [Cl $^{-}$ ] in the range 0.1–5.0 mol L $^{-1}$ . The solutions used were prepared with Type I water, reagent-grade sodium sulphide (Na $_2$ S·9H $_2$ O, 98.0% assay), and reagent-grade sodium chloride (NaCl, 99.0% assay). Electrodes were immersed in the [SH $^{-}$ ] solutions (1L) for various times under natural corrosion conditions. A standard three-electrode system was employed with a Pt plate as the counter electrode and a saturated calomel electrode (SCE) as the reference electrode. All potentials, unless otherwise specified, are quoted on this scale. Before each experiment, electrodes were cathodically cleaned at  $-1.6$  V/SCE for 2 min, and then at  $-1.15$  V/SCE for 2 min.

Because of the long duration of experiments, it was necessary to periodically monitor the [SH $^{-}$ ] over the course of an experiment. As demonstrated previously, the pH of a SH $^{-}$  solution can be used to monitor the [SH $^{-}$ ]. Consequently, the pH was recorded weekly, and SH $^{-}$  added, when required, to readjust its concentration to the original value [7].

Experiments were performed at ambient temperature,  $25 \pm 2^\circ\text{C}$ . The corrosion potential ( $E_{\text{CORR}}$ ) was monitored, and electrochemical impedance spectroscopy (EIS) measurements were performed at  $E_{\text{CORR}}$  using a Solartron 1287 electrochemical interface and a Solartron 1255B frequency response analyser. A sinusoidal potential perturbation with an amplitude (peak-to-zero) of 10 mV was applied over the frequency range from  $10^5$  to  $10^{-3}$  Hz. Data were obtained at 10 frequencies per decade. The validity of the impedance spectra was checked using the Kramers–Kronig transform.

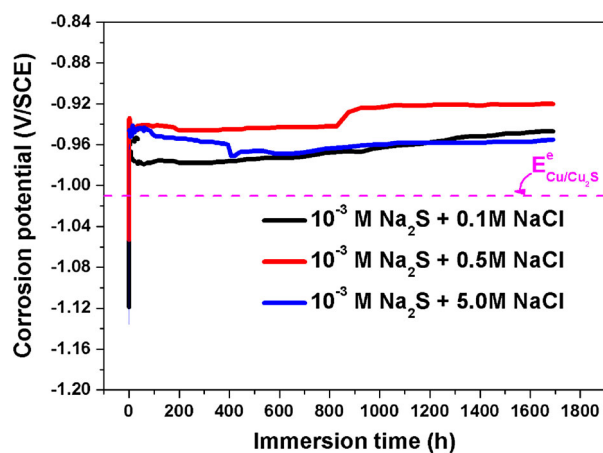


**Figure 1.** Evolution of  $E_{\text{CORR}}$  of copper with immersion time in  $10^{-3}$  mol L $^{-1}$  sulphide containing chloride in the concentration range of 0.1–5.0 mol L $^{-1}$ .

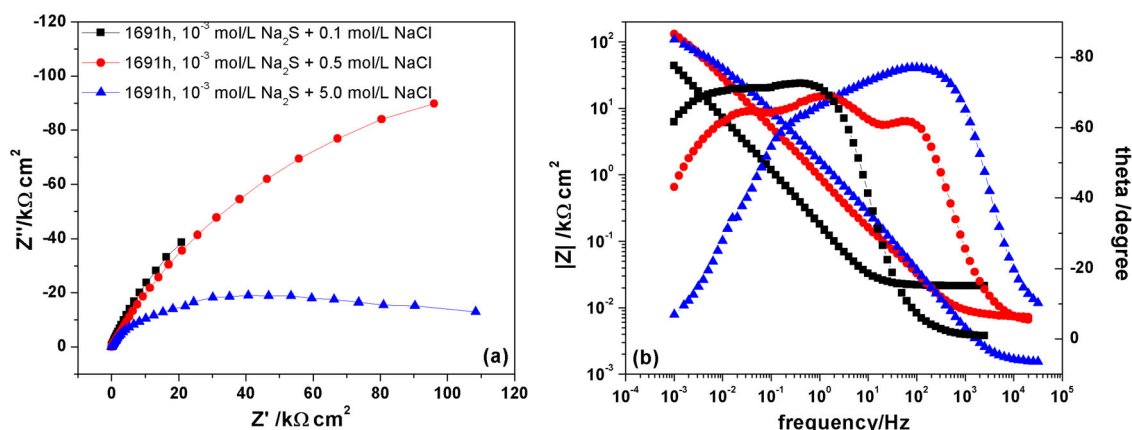


**Figure 2.** Nyquist (a) and Bode (b) plots on copper after 1691 h immersion in: (■) anoxic  $10^{-3}$  mol L $^{-1}$  Na $_2$ S + 0.1 mol L $^{-1}$  NaCl solution; (●) anoxic  $10^{-3}$  mol L $^{-1}$  Na $_2$ S + 0.5 mol L $^{-1}$  NaCl solution; and (▲) anoxic  $10^{-3}$  mol L $^{-1}$  Na $_2$ S + 5.0 mol L $^{-1}$  NaCl solution.

## Surface and solution analyses

Electrodes removed from solution for surface analyses were rinsed with Type I water for 10 min and dried with cold Ar gas. Analyses were then performed immediately with the minimum period of interim storage (<30 min). The surface and cross-sectional morphologies of corroded specimens were observed using a Leo 1540 scanning electron microscope (SEM) equipped with a focused ion beam (FIB) (Zeiss Nano Technology Systems Division, Germany). The composition of sulphide films was qualitatively analysed by energy dispersive X-ray spectroscopy (EDS) using a Leo 1540 FIB/SEM microscope. The Cu content of solutions was analysed using plasma atomic emission spectroscopy (ICP-AES). Analyses were performed within two weeks to avoid conversion of the copper sulphide to insoluble copper oxide in the acidified sample used for the analysis.

## Results and discussion

### $E_{\text{CORR}}$ and EIS measurements

Cu electrodes were immersed in  $10^{-3}$  mol L $^{-1}$  Na $_2$ S solutions containing different Cl $^{-}$  contents in the range from 0.1 to 5.0 mol L $^{-1}$  for an exposure time up to 1691 h (~71 days). Over this exposure period,  $E_{\text{CORR}}$  was monitored continuously with the rapidly attained steady-state  $E_{\text{CORR}}$  being independent of [Cl $^{-}$ ] within the range  $\sim -960 \pm 20$  mV/SCE, Figure 1. This value is close to the equilibrium potential for Cu/Cu $_2$ S at this [SH $^{-}$ ] ( $-1.01$  V/SCE), suggesting that the corrosion film deposited on the Cu surface was Cu $_2$ S, as demonstrated previously by XRD [7].

When [Cl $^{-}$ ] was low (i.e. 0.1 mol L $^{-1}$ ), EIS spectra exhibited two time constants attributable to the formation of Cu $^{+}$  species at the Cu/Cu $_2$ S interface and the impedance properties of the Cu $_2$ S film (Figure 2(a)). With time, the resistance at the low frequency limit increased, consistent with the thickening of an, at least partially, protective film. When the [Cl $^{-}$ ] was increased to 0.5 mol L $^{-1}$  the EIS spectra exhibited three time constants indicating a clear influence of Cl $^{-}$  on the properties of the film. The detection of a high frequency response, Figure 2(b), implied the charge transfer process at the Cu/Cu $_2$ S interface was accelerated suggesting porosity in the film. A further increase in [Cl $^{-}$ ] (to 5.0 mol L $^{-1}$ ) also yielded EIS spectra with three time constants with the high frequency response shifting to even higher frequencies,

consistent with the presence of open porosity in a non-protective  $\text{Cu}_2\text{S}$  film. Despite this apparent increase in porosity the impedance at the low frequency limit remained almost unchanged. A more detailed analysis of this impedance study will be published elsewhere.

### Surface and cross-sectional morphologies of $\text{Cu}_2\text{S}$ film

The surface morphologies of the  $\text{Cu}_2\text{S}$  films formed after 1691 h immersion in  $10^{-3} \text{ mol L}^{-1} \text{ Na}_2\text{S}$  solution containing different  $[\text{Cl}^-]$  are shown in Figure 3. In  $\text{SH}^-$  solutions containing  $0.1 \text{ mol L}^{-1} \text{ Cl}^-$ , well-defined  $\text{Cu}_2\text{S}$  crystals were formed and grew rapidly as corrosion continued, some up to  $\sim 20 \mu\text{m}$  in dimension after 1691 h, Figure 3(a). For a  $[\text{Cl}^-]$  of  $0.5 \text{ mol L}^{-1}$ , the surface also became covered with a crystalline film but with crystals with much smaller dimensions than that formed at the lower  $[\text{Cl}^-]$  over the same immersion period (Figure 3(b)).

When the  $[\text{Cl}^-]$  was increased to  $5.0 \text{ mol L}^{-1}$ , Figure 3(c), the  $\text{Cu}_2\text{S}$  film grew rapidly but two-dimensionally and with a high porosity. Subsequently, for interim exposure periods (not shown here), the pores became blocked with agglomerates of nanoparticles. However, over the extended exposure period (1691 h) these particulates were either lost or re-dissolved. The formation and subsequent disappearance of these particulates suggests Cu was mobile in extremely saline solutions, a process which appears to be attributable to the variation in chemical conditions within the rapidly grown porous film. We have speculated that this could be attributed to the formation of  $\text{CuCl}_2^-$  soluble complexes which allowed transport of  $\text{Cu}^+$  out of the pores before precipitation of Cu-sulphide clusters. That Cu transport occurred in this concentrated  $\text{Cl}^-$  solution was confirmed by analyses of the solution which showed concentrations of 520 ppb. Analyses after the experiments at lower  $[\text{Cl}^-]$  detected no soluble Cu (detection limit 4 ppb).

The mode and form of Cu transport has been addressed elsewhere [11].

Figure 4 shows cross-sections cut using FIB after 1691 h of immersion in the three different  $\text{Cl}^-$  solutions. It is clear that the  $\text{Cu}_2\text{S}$  deposit was comprised of a single layer in all cases. At the lowest  $[\text{Cl}^-]$  the film is compact and protective, Figure 4(a) as indicated by the EIS measurements. As the  $[\text{Cl}^-]$  was increased the film became increasingly more porous, Figure 4(b,c), again consistent with the EIS measurements.

### Film growth kinetics

Besides influencing the morphology and porosity, the  $[\text{Cl}^-]$  influenced the film growth rate, the film thickness decreasing as  $[\text{Cl}^-]$  increased, suggesting  $\text{Cl}^-$  inhibited the film growth process. Because the deposits are non-uniform, the thickness varies with location. Consequently, film thicknesses were measured at various locations and the variability represented in the plots by the standard deviations. This procedure yielded a reasonable measure of film growth kinetics at the two lowest  $[\text{Cl}^-]$  but not at the highest concentration for which the apparent film thickness was not representative of film growth kinetics due to the high porosity and the loss of Cu to the solution.

In general, the film growth kinetics can be empirically described by the power law [7,8]

$$d = At^n \quad (1)$$

where  $d$  is the corrosion film thickness,  $A$  is a constant, and  $n$  is the time exponent. The parameter  $A$  can be taken to be the initial film growth rate when  $n < 1$  or the average film growth rate when  $n = 1$ , and  $n$ , usually in a range of 0.5–1.0, as an indicator of the protectiveness of the corrosion products formed. The lower the value of  $n$ , the more protective the corrosion film.

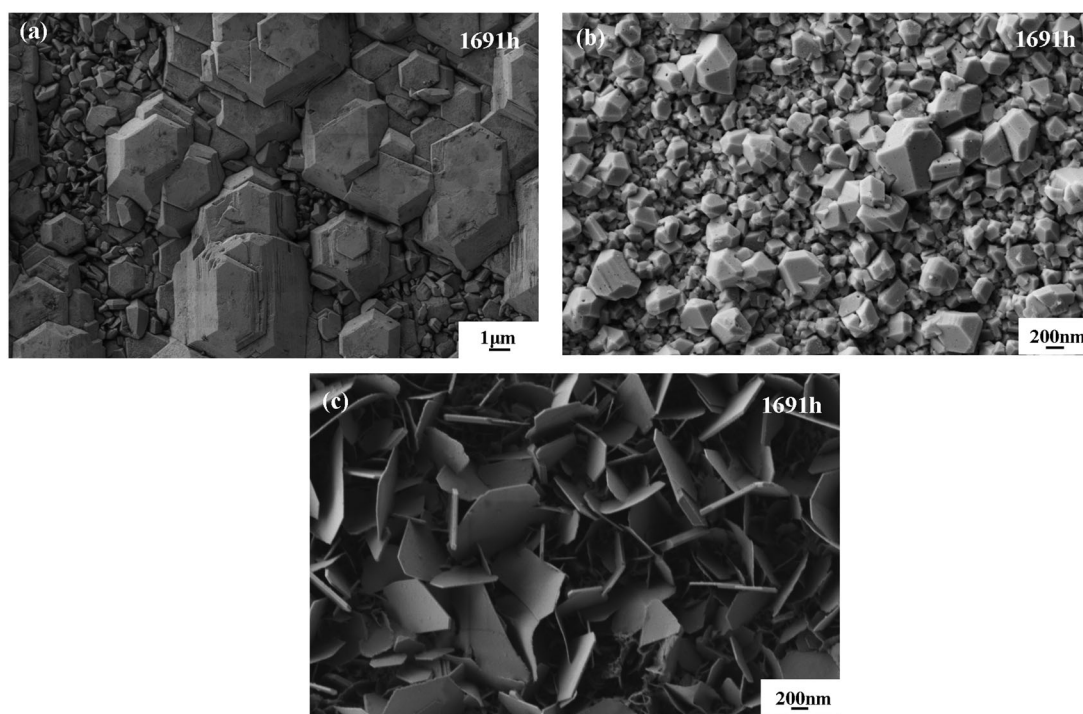


**Figure 3.** Morphology of the  $\text{Cu}_2\text{S}$  film formed on Cu after 1691 h immersion in: (a)  $1 \times 10^{-3} \text{ mol L}^{-1} \text{ Na}_2\text{S} + 0.1 \text{ mol L}^{-1} \text{ NaCl}$  solution; (b)  $1 \times 10^{-3} \text{ mol L}^{-1} \text{ Na}_2\text{S} + 0.5 \text{ mol L}^{-1} \text{ NaCl}$  solution; and (c)  $1 \times 10^{-3} \text{ mol L}^{-1} \text{ Na}_2\text{S} + 5.0 \text{ mol L}^{-1} \text{ NaCl}$  solution.

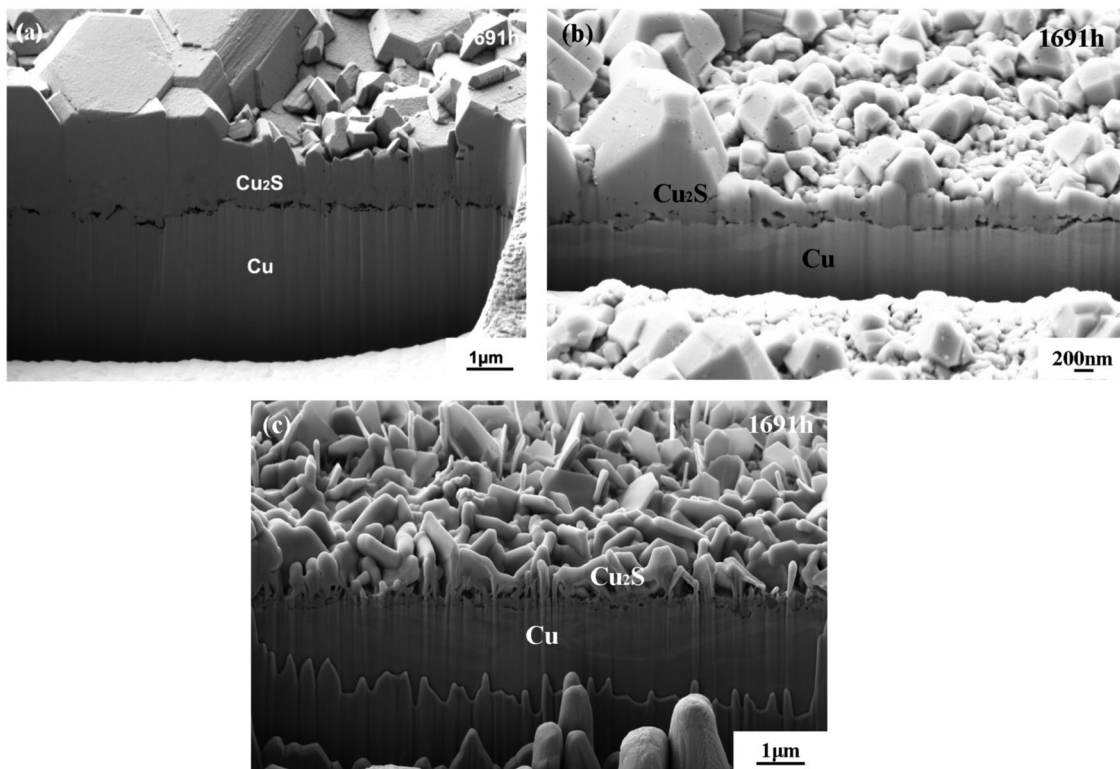


**Figure 4.** FIB cut cross-sections of the  $\text{Cu}_2\text{S}$  film formed on Cu after 1691 h immersion in: (a)  $1 \times 10^{-3} \text{ mol L}^{-1} \text{ Na}_2\text{S} + 0.1 \text{ mol L}^{-1} \text{ NaCl}$  solution; (b)  $1 \times 10^{-3} \text{ mol L}^{-1} \text{ Na}_2\text{S} + 0.5 \text{ mol L}^{-1} \text{ NaCl}$  solution; and (c)  $1 \times 10^{-3} \text{ mol L}^{-1} \text{ Na}_2\text{S} + 5.0 \text{ mol L}^{-1} \text{ NaCl}$  solution.

Figure 5 shows the evolution of the corrosion film thickness as a function of immersion time for the two lower  $[\text{Cl}^-]$ s. For  $[\text{Cl}^-] = 0.1 \text{ mol L}^{-1}$ , the film growth kinetics obey a parabolic law, a linear least squares fit to the data yielding values for  $A$  and  $n$  of 58 and 0.5, respectively, with a fitting dependency of  $>0.98$ . This parabolic growth law suggests the diffusive  $\text{SH}^-$  flux was larger than the interfacial film formation rate consistent with control of the film growth process by  $\text{Cu}^+$  diffusion in the film [7,9], as suggested by the EIS results.

When the  $[\text{Cl}^-]$  was increased to  $0.5 \text{ mol L}^{-1}$ , the  $\text{Cu}_2\text{S}$  film grew linearly with immersion time. The linear fit to the data in Figure 3 yields values for  $A$  of 0.226, with a fitting dependency of  $>0.98$ . According to our previous work [8], this corresponds to an average film growth rate of  $\sim 1.98 \mu\text{m}/\text{year}$ . The linear increase in film thickness with immersion time

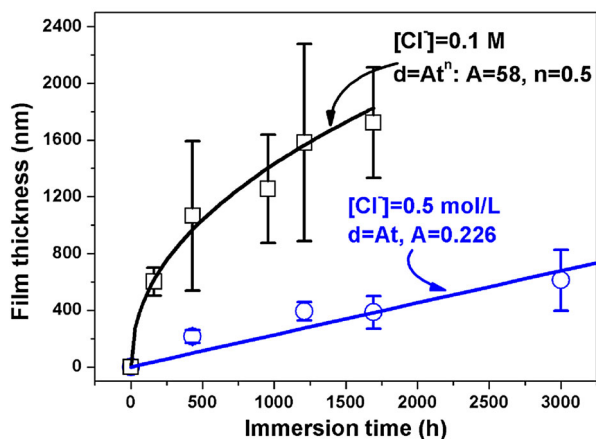


**Figure 5.** Sulphide film growth laws on Cu in anaerobic sulphide solutions containing different chloride concentrations.

indicates that the corrosion film was not protective over this time period ( $\sim 125$  days), with the interfacial reaction rate being larger than the diffusive  $\text{SH}^-$  flux. Under this condition, the Cu content in solution was below the detection limit, indicating that Cu degraded by sulphide is completely sequestered as corrosion product deposited on the Cu surface. Thus, the decrease in film growth rate despite the increased film porosity may be attributable to the ability of  $\text{Cl}^-$  to displace adsorbed  $\text{SH}^-$  from the exposed Cu surface at the base of the pores, the essential first step in the overall corrosion process. A detailed electrochemical investigation of the anodic reaction is under way.

## Conclusions

The properties and structure of sulphide films formed by corrosion on Cu surfaces were investigated in stagnant, anaerobic  $10^{-3} \text{ mol L}^{-1}$  sulphide solutions containing different chloride contents in the range  $0.1\text{--}5.0 \text{ mol L}^{-1}$ . The main conclusions drawn were as follows:

- At low  $[\text{Cl}^-]$  ( $0.1 \text{ mol L}^{-1}$ ), the  $\text{Cu}_2\text{S}$  film was protective and exhibited a parabolic growth law.
- At a higher  $[\text{Cl}^-]$  of  $0.5 \text{ mol L}^{-1}$ , EIS data indicate the  $\text{Cu}_2\text{S}$  film was porous. This was confirmed by micrographs on FIB cut cross-sections. The film grew linearly with time indicating it was not protective.
- At a very high  $[\text{Cl}^-]$  ( $5.0 \text{ mol L}^{-1}$ ), the  $\text{Cu}_2\text{S}$  film grew two-dimensionally with extensive porosity. The film growth process appeared to be controlled by a combination of  $\text{SH}^-$  diffusion in the bulk of the solution and  $\text{CuCl}_2^-$  in the pores of the cellular sulphide film. Solution analyses confirmed that Cu was released to the bulk solution.

- (iv) Chloride influences the  $\text{Cu}_2\text{S}$  film growth process in a number of ways: (a) it displaces adsorbed  $\text{SH}^-$  from the Cu surface thereby inhibiting the critical first step in the corrosion process; (b) it induces and maintains porosity in the film; (c) at extremely high concentrations it facilitates transport of Cu into the solution possibly by transport as  $\text{CuCl}_2^-$  in the pores in the film and as Cu-sulphide complex/clusters in the bulk solution.

### Acknowledgements

The authors would like to thank Dr T. Simpson for his help with SEM/FIB, and Christina Lilja (SKB) and Fraser King (Integrity Corrosion Consulting, Nanaimo, BC, Canada) for many helpful discussions.

### Disclosure statement

No potential conflict of interest was reported by the authors.

### Funding

This research was funded by Svensk Karnbranslehantering AB (Stockholm, Sweden) and Posiva Oy (Olkiluoto, Finland).

### References

- [1] Shoesmith DW. Assessing the corrosion performance of high-level nuclear waste containers. *Corrosion*. 2006;62:703–722.
- [2] Féron D, Crusset D, Gras JM. Corrosion issues in nuclear waste disposal. *J Nucl Mater*. 2008;378:16–23.
- [3] King F, Kolar M, Maak P. Reactive-transport model for the prediction of the uniform corrosion behavior of copper used fuel containers. *J Nucl Mater*. 2008;379(1–2):133–141.
- [4] King F, Lilja C, Pedersen K, et al. An update of the state-of-the-art report on the corrosion of copper under expected conditions in a deep geologic repository. SKB Technical Report, 2010, TR-10-67.
- [5] Pedersen K. Microbial processes in radioactive waste disposal, SKB Swedish Nuclear Fuel and Waste Management Co. Technical Report, TR-00-04, 2000.
- [6] Chen J, Qin Z, Shoesmith DW. Copper corrosion in aqueous sulphide solutions under nuclear waste repository conditions, scientific basis for nuclear waste management XXXV (Buenos Aires, Argentina, Oct 2–7, 2011), MRS Proceedings 1475, imrc11-1475-nw35-o16.
- [7] Chen J, Qin Z, Shoesmith DW. Kinetics of corrosion film growth on copper in neutral chloride solutions containing small concentrations of sulfide. *J Electrochem Soc*. 2010;157(10):C338–C345.
- [8] Chen J, Qin Z, Shoesmith DW. Long-term corrosion process of copper in anaerobic low sulfide solution. *Electrochim Acta*. 2011;56:7854–7861.
- [9] Chen J, Qin Z, Shoesmith DW. Key parameters determining structure and properties of sulphide films formed on copper corroding in anoxic sulphide solutions. *Corros Eng Sci Technol*. 2014;49:415–419.
- [10] Chen J, Qin Z, Wu L, et al. The influence of sulphide transport on the growth and properties of copper sulphide films on copper. *Corros Sci*. 2014;87:233–238.
- [11] Chen J, Qin Z, Martino T, et al. Non-uniform film growth and micro/macro-galvanic corrosion of copper in aqueous sulphide solutions containing chloride. *Corros Sci*. 2017;114:72–78.